Technoeconomic Analysis of a Waste Tire to Liquefied Synthetic Natural Gas (SNG) energy system

Avinash S.R. Subramanian[a], Truls Gundersen[a], Thomas A. Adams II[b]

[a]*Department of Energy and Process Engineering, Norwegian University of Science and Technology (NTNU), Kolbjørn Hejes vei 1B, NO-7491, Trondheim, Norway.*
[b]*Department of Chemical Engineering, McMaster University, 1280 Main St. W, Hamilton, ON, Canada, L8S 4L7.*

Abstract

Thermochemical conversion of solid wastes through gasification offers the dual benefit of production of high-value fuels and environmentally friendly waste disposal. In this paper, we propose a novel process for production of liquefied synthetic natural gas (SNG) from waste tires via a rotary kiln gasification process. We use a combination of experimental data available in the open literature, first principles mathematical models and empirical models to study three design cases (without CO_2 Capture and Sequestration (CCS), with precombustion CCS and with pre- and postcombustion CCS) in two locations (USA and Norway). The thermodynamic, economic and environmental performance of the concept is studied. The results show that minimum selling prices of 16.7, 17.5 and 19.9 \$/GJ$_{LHV,SNG}$ are required for USA and 20.9, 21.8 and 24.9 \$/GJ$_{LHV,SNG}$ for Norway. We note that these prices may become competitive under certain regulatory conditions (such as recent public policy movement in British Columbia, Canada requiring public utilities to purchase natural gas made from renewables at prices up to 30 \$/GJ$_{LHV,SNG}$). The minimum selling price reduces substantially with process scale and with levying tipping fees. The design situated in Norway with both pre- and post-combustion CCS has near zero direct and indirect CO_2 emissions.

Keywords: Waste-to-Energy, Waste tire, Gasification, CO_2 capture and sequestration (CCS), Synthetic Natural Gas (SNG), Rubber

1. Introduction

The growing global demand for energy is motivating research efforts both to utilize alternative feedstocks such as solid wastes (waste tires, plastics and municipal solid waste) as well as to develop efficient and environmentally sustainable conversion processes. Concurrently, increased population growth creates large quantities of wastes that require appropriate management. Thermochemical conversion processes, such as gasification, are promising options that offer the dual benefit of both recovery of high-value products from these solid wastes as well as their environmentally friendly disposal. Belgiorno et al. suggest that homogeneous high-energy density wastes such as waste tires are particularly suitable for gasification as a result of their high volatile matter content ($\sim$ 67%), low ash content ($\sim$ 7%) and high calorific value (LHV of $\sim$ 33.96 MJ/kg, higher than coal) [1]. In the developed world, approximately 1 waste tire per person per year is produced resulting in approximately 1 billion discarded tires annually [2]. In addition, there are currently an estimated 4 billion waste tires in landfills and stockpiles worldwide highlighting the extent of the disposal problem. Previous waste tire management strategies have aimed at either material recovery or energy recovery as reviewed in [3]. The use of gasification as an alternative conversion process allows for both material and energy recovery through the production of higher value products through the syngas route.

However, research into waste tire gasification has been limited and mainly focussed on bench scale experimental studies as reviewed by Labaki and Jeguirim [4] and Oboirien and North [5]. Several gasifier types have been studied including fixed bed, fluidized bed, entrained flow and rotary kiln gasifiers. These gasifier types have different levels of suitability for waste tire conversion. For each type, syngas yield and composition is influenced by various operating parameters including: type and flowrate of the oxidizing agent (e.g., oxygen, steam, or CO_2), gasifier temperature and pressure, flow regime (downflow, upflow, circulating) and the mode of heating (indirect or direct firing). Fixed bed reactors may be suitable for small-scale processes [6] and their use has been investigated for producing hydrogen-rich syngas by Elbaba et al. ([7]) and Elbaba and Williams ([8], [9]). Fluidized beds may be suitable for large-scale processes but are generally fairly expensive and require expensive external tar cracking and particulate removal [6]. In addition, experimental results on syngas yields and composition from fluidized bed gasifiers by Karatas et al. ([10], [11]) and Wang and Leung ([12],

[13]) have been inconsistent. Entrained flow (EF) gasification, with essentially the same gasifier design used commercially for coal gasification, is a highly efficient, high temperature process that has the substantial advantage of complete tar cracking and removal from the syngas generated [14]. In addition, recent research has shown the value of using EF gasifiers with tight heat integration for processes utilizing multiple feedstocks such as coal and natural gas [15], [16], petcoke and natural gas [17], and biomass and natural gas [18]. However, EF gasification is fairly expensive, imposes tight restrictions on feedstock quality, and requires additional units for feedstock and slurry preparation and feeding [6],[14]. Despite these drawbacks, Larson et al. [14] and Boerrigter and Van der Drift [19] recommend EF gasification for large-scale biomass conversion. However, to the best of the authors' knowledge, no experimental data on EF gasification of waste tires is available in the open literature. Thus, investigation of the potential of EF gasification is left as future work where the following issues will be studied: Deterministic global process optimization (with several decision variables including gasifier operating conditions and choice of various possible products) [20], optimal design considering the inclusion of natural gas as a second feedstock to give syngas streams of different qualities that can be blended [21], optimal design and operation under uncertainty of a flexible polygeneration process using a stochastic programming approach solved using decomposition algorithms [22], [23].

Rotary kiln gasifiers are a mature technology used commercially in several applications (such as cement production [24]). They consist of a downward-sloping rotating drum into which the waste and the oxidizing agent are fed. Heat is provided by either direct firing, when combustion takes place within the drum, or indirect firing when the drum is housed within a furnace. Amodeo et al. suggest that rotary kilns are particularly suited for solid wastes because they allow a wider range of feed particle sizes, compositions and densities and are less sensitive to feed moisture content (allowing up to 50 %) [25]. In addition, rotary kilns have minimal maintenance requirements and sufficient turndown capacity, produce syngas with consistent quality and low tar content, and can handle difficult wastes such as waste tires. Despite these potential advantages, rotary kiln gasifiers have not received much research attention particularly from the systems perspective. Robust experimental results were obtained by researchers at the Italian National Agency for New Technologies (ENEA) who conducted several studies on steam gasification in a rotary kiln at temperatures between 850 - 1000 °C. The syngas

produced contained mostly H_2 (50 - 65 %v/v) and significant CH_4 (10 - 30 %v/v), CO (8 - 21 %v/v), C_2H_4 (0 - 10 %v/v) and CO_2 (2 - 8%v/v) with the overall gas yield increasing with temperature [26], [27]. However, all experiments were run at atmospheric pressure which may not be favorable for large-scale processes as expensive syngas compression may be required prior to downstream synthesis [14]. In addition, significant amounts of tar and particulate matter were reported in the syngas thus requiring an expensive external tar cracker and ceramic filter. Despite these drawbacks, we use rotary kiln gasification in this work because of the advantages mentioned and the availability of robust experimental data.

The different gasifier configurations result in different syngas qualities with a range of H_2:CO ratios. Depending on the ratio obtained, syngas could be used for production of fuels (such as diesel, gasoline, synthetic natural gas (SNG) and hydrogen), chemicals (such as methanol, dimethyl ether (DME), ethanol, and olefins), or electricity. The syngas could also produce multiple of these products as part of a polygeneration scheme [28]. In this work, considering that tire-derived syngas in rotary kilns has a high H_2:CO ratio of 3.77, we investigate the production of SNG. Haldor Topsøe's TREMP methanation process is used to convert syngas to SNG [29]. This process does not require an exact H_2:CO ratio of 3.0; in order to compensate for the excess H_2 and maximize conversion to SNG, a small amount of CO_2 is left in the syngas as explained in Section 2.2.2. This eliminates the need for an inefficient reverse water gas shift step. The decision to produce SNG was also influenced by the Norwegian context in which natural gas exports are expected to have an increasing share of revenue earned. Liquefaction of SNG enables the product to be sold on the fast-growing global LNG market as well as to utilize existing Norwegian LNG supply chain infrastructure. Furthermore, the highest demand growth for natural gas is expected to arise from China and South-East Asia [30]. Thus, transportation of liquefied SNG from Norway is typically the more suitable option compared to building pipelines. We use the Poly-Refrigerated Integrated Cycle Operations (PRICO) (or Single Mixed Refrigerant (SMR)) process for liquefaction because it is the simplest and most researched commercial process [31].

Promising studies are available in the literature for production of SNG from biomass. For instance, Batidzirai et al. investigated the thermodynamic, economic, and environmental performance of the entire biomass-based SNG supply chain [32]. Van der Meijden et al. studied wood to SNG systems using different types of gasifiers [33]. Zwart et al. analyzed the potential of

bioSNG production in a integrated system with the aid of a bench scale set-up [34]. Gassner and Maréchal studied a variety of thermo-conversion options for biomass to SNG including indirect and direct-heated gasification [35]. Further, the optimal design strategies for polygeneration of SNG, power and heat were investigated [36].

However, to the authors' knowledge, there have been no research efforts analyzing waste tire to liquefied SNG processes. Therefore the objective of this paper is to evaluate the thermodynamic, economic and environmental performance of the proposed waste tire to liquefied SNG concept from the systems perspective at industrially relevant scales. While other gasifier configurations (such as fixed-bed, fluidized-bed and entrained-flow) have received research attention, rotary kilns have not been studied. Accurate modeling of the gasifier is a challenging task, thus in this work we used a combination of experimental data (from [27]) and commercial process simulation software to perform the analysis and validate the results. All the unit operation models consist of mass and energy balances based on first-principles and thus do not require tuning or fitting of parameters. Instead, the fundamental uncertainty lies in physical property models. However, we have carefully chosen the physical property models such that they accurately represent experimental data (such as critical Vapour-Liquid Equilibrium data). For this reason, the whole simulation is based on the best possible knowledge one can have without building the plant itself. We also note that several studies that consider SNG as a product do not incorporate a final liquefaction step. It is our proposition that liquefaction is essential to enable the product to access global supply chains and be sold on the international market especially since a substantial portion of future demand is expected to arise from China and South-East Asia.

Three designs (without CCS, with precombustion CCS and with pre- and postcombustion CCS) are studied as illustrated in Figure 1. Two plant locations are considered: USA and Norway. Furthermore, the influence of the process scale, tipping fees and CO_2 tax rates on economic performance is determined by means of a sensitivity analysis. Finally, the relative impact of certain economic and process parameters on the minimum selling price is illustrated using a tornado plot.

2. Methodology

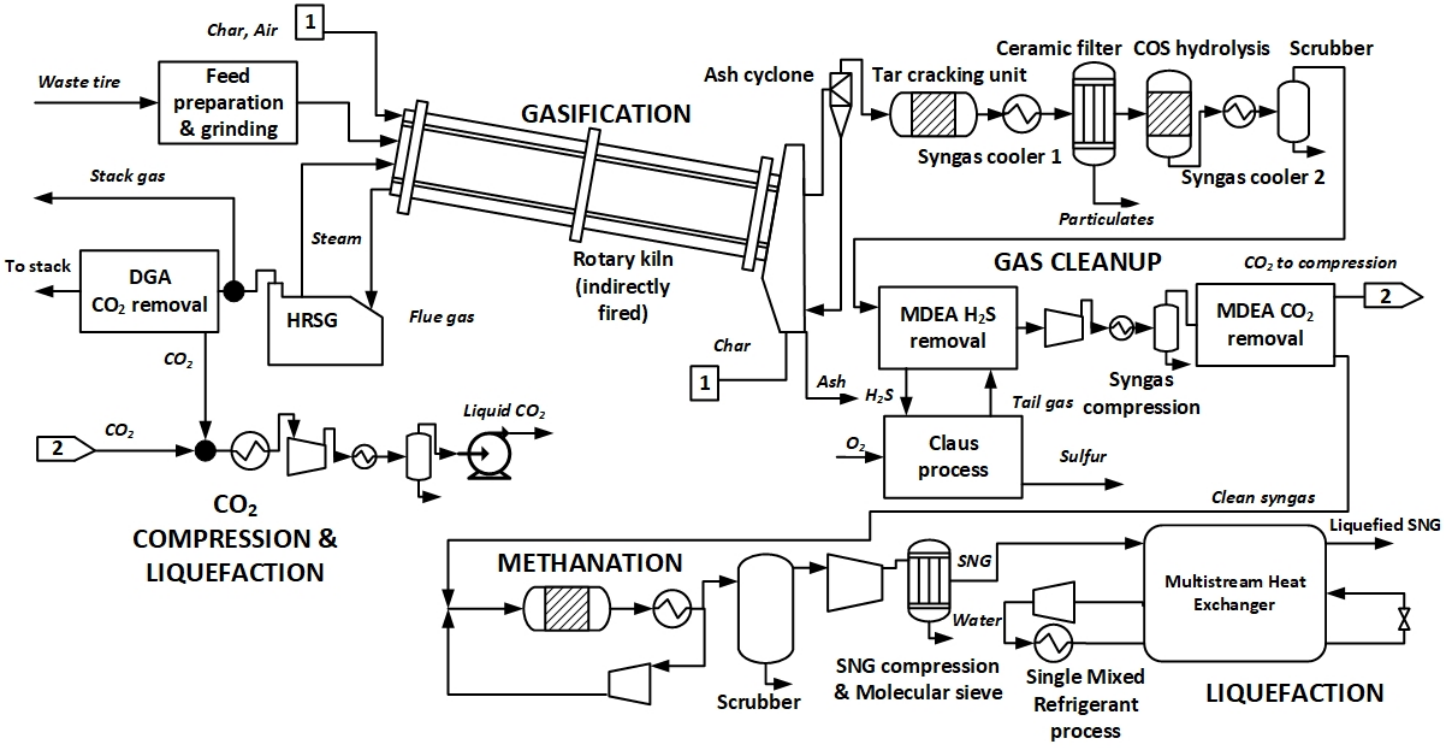

Figure 1: Detailed process flow diagram for the waste tire to liquefied synthetic natural gas (SNG) process

2.1. Simulation basis

Figure 1 illustrates the major sections of the proposed waste tire to liquefied synthetic natural gas process. Three design cases are studied. For the case without CO_2 capture, the waste tire is gasified with steam in a rotary kiln to generate syngas that undergoes cleaning using a two-stage MDEA process to remove H_2S and CO_2 before heading to the downstream synthesis section. The captured H_2S stream is converted to elemental sulfur in a Claus process, while the CO_2 is emitted. Heat for the gasification is provided by housing the kiln in a furnace in which combustion of the unreacted char occurs, with the resulting flue gas emitted. The cleaned syngas is then converted to methane in the methanation section. The methane is then compressed before heading to the liquefaction section where it exits as liquefied SNG. The second case with pre-combustion CO_2 capture features essentially the same units, except that the CO_2 captured in the MDEA process is compressed and liquefied for sequestration. Similarly, the case with both pre and post-combustion CCS features all the above units except that the flue gas stream passes through a cleaning process with Diglycol Amine (DGA) to capture CO_2, which then heads to the CO_2 compression and liquefaction section.

These three concepts are analyzed using a combination of commercial process simulation software and experimental data available from the literature. Mass and energy balances for most of the unit operations are developed using Aspen Plus v10, except for the MDEA-based H_2S and CO_2 removal sections that are modeled using BR&E's ProMax v4. For physical property calculations, the Peng-Robinson equation of state with the Boston-Mathias modification (PR-BM) was used for the gasification, Claus, CO_2 compression, and SNG liquefaction sections in order to be consistent with previous work [16], [17]. The Redlich-Kwong-Soave equation of state with modified Huron-Vidal mixing rules is used for the methanation section as validated in [37]. The Amine package in ProMax was used for the H_2S and CO_2 removal sections consistent with previous work [17]. The ElecNRTL package in Aspen Plus is used for the DGA-based CO_2 capture process [38]. For the complex gasification process, experimental results published by Portofino et al. [27] are used to specify the syngas yield and composition.

The waste tire feedstock is assumed to be identical to that studied in [27] with respect to proximate and ultimate composition, as illustrated in Table 1. The liquefied SNG produced contains at least 99.5 mol% CH_4. The Aspen Plus simulation contained the following conventional components: CO, CO_2, H_2, H_2O, N_2, AR, CH_4, H_2S, O_2, NO, NO_2, SO_2, SO_3, COS, CH_3OH, C_2H_6,

C_2H_4, C_3H_8, i-C_4H_{10}, n-C_4H_{10}, i-C_5H_{12}, and n-C_5H_{12}, S_2, S_3, S_4, S_5, S_6, S_7, S_8, DGA, DGA^+, H_3O^+, $DGACOO^-$, OH^-, $HCO_3{}^-$, $CO_3{}^{2-}$. Solids: C and S, and Nonconventional solids: Waste tire, Char, Tar, Soot and Ash. Table 2 presents a summary of the operating parameters and assumptions of the simulation. The three concepts are scaled such that the thermal input of the waste tire feedstock is 893 MW_{LHV} (equivalent to approximately 26.3 kg/s of waste tire) in order to be consistent with previous studies [14].

Ultimate Analysis	**wt %**	**Proximate Analysis**	**wt %**
C	77.3	Volatile Matter	67.7
H	6.2	Fixed Carbon	25.5
N	0.6	Ash	6.8
S	1.8		
O	7.3		
LHV [MJ/kg]	33.96		

Table 1: Characterization of waste tire

Unit	Parameters	Reference
Waste tire preparation	Crumb tire size = 6.0 mm	[27],[39]
Rotary kiln gasifier	Rotary kiln steam gasification. 66.7 wt% steam/33.3wt% waste tire	
	T = 1000 °C, P = 1.013 bar	[27]
Furnace	T = 1050 °C, P = 1.013 bar	Assumed
COS hydrolysis	T = 200 °C, P = 1.013 bar	
H_2S removal	Solvent composition: 50.0 wt% MDEA: 50.0 wt% H_2O	[38]
	T = 45 °C, P = 1.013 bar, Removal: 96.2 %	
CO_2 removal	Solvent composition: 45.0 wt% MDEA: 5.0 wt% piperazine: 50.0 wt% H_2O,	[38]
	T = 45 °C, P = 23 bar, Removal: 88.2 %	-
Claus process	Two-stage sulfur conversion, Furnace: T = 950 °C	[40]
Methanation	Four-stage conversion, Inlet T = 300 °C, Inlet P = 23 bar. ΔP = 3 bar	[41]
	Recycle rate = 75 %	
SNG compression & purification	Outlet pressure = 55 bar, Molecular sieve removes 98.5% CO_2 and all H_2O	[40]
SNG liquefaction	SNG flowrate = 9.7 kg/s, P = 55 bar, Inlet T = 22 °C, Outlet T = -157 °C	[31]
	SNG Mole composition: CH_4: 99.4 %, H_2: 0.5 %, CO_2: 0.03 %	
	MSHE UA_{max} = 25.0 MW/K, Pressure ratio = 6.47	
	Refrigerant:	
	Mole compostion: N_2: 8.32, CH_4: 24.02, C_2H_6: 36.88, C_3H_8: 0.00, n-C_4H_{10}: 30.77	
	Low P = 2.79 bar, high P = 18.04 bar, Δ T_{min} = 0.95 K, Flowrate = 58.5 kg/s	
CO_2 compression	Multistage compressors CO_2 purity = 99.1 %, Outlet T = 25 °C, P = 153 bar	[42]
Postcombustion CO_2 capture	Solvent composition: 72.3 wt% DGA: 27.3 wt% H_2O	[38]
	T = 70 °C, P = 1.0 bar, CO_2 Removal = 95.0 %	
Compressors	Isentropic efficiency = 80 %, maximum pressure ratio = 5	[16]
Pumps	Isentropic Efficiency = 80 %	[16]
Heat Exchanger Network	ΔT_{min} = 5 °C, Maximum 10 branch splits per stream	[17], AEA
	Utilities:	
	Cooling water: T_{in} = 10 °C, T_{out} = 16 °C, Cost = 5.15e-9 $\$_{2016}$/kJ	AEA
	LP steam generation: T = 125 °C, P = 1.2 bar, Cost = 1.89e-6 $\$_{2016}$/kJ	Assumed
	MP steam : T = 300 °C, P = 12 bar, Cost = 2.20e-6 $\$_{2016}$/kJ	[17]
	HP steam generation: T = 480 °C, P = 50 bar, Cost = 2.49e-6 $\$_{2016}$/kJ	[17]

Table 2: Operating parameters and specifications of the simulation

2.2. Case 1: Without CCS

2.2.1. Rotary kiln gasification

Waste tires received at the plant gate are shredded and ground to a maximum size of 6 mm to meet the specifications suggested by Portofino et al. [27], [39]. The resulting crumb tire together with steam is fed to the rotary kiln gasifier. The gasification phenomena include pyrolysis, devolatilization, char gasification, sulfur reaction, and a complex series of chemical reactions to give a gaseous product (consisting primarily of H_2, CO, CH_4 and CO_2), tar and soot, and unreacted char as shown in Table 3 [27], [43]. The gasifier is operated at 1000 °C and 1.013 bar because experimental results at these operating conditions produced the highest gas yield as shown in Table 3 [27].

Product	**Yield** [kg/kg_{feed}]	**Composition**
Raw syngas	2.62	**Mole fractions**:
		H_2O: 0.416, CH_4: 0.048
		H_2: 0.309, CO_2: 0.136
		CO: 0.082, COS: 0.003
		C_2H_4: 0.002, C_2H_6: 0.002
Char	0.33	**Proximate Analysis**:
		Volatile Matter: 5.65
		Fixed Carbon 71.99
		Ash: 21.92

Table 3: Yield and composition of products of steam gasification at 1000 °C and 1.013 bar obtained from [27]

The experimental results for the syngas composition are incorporated in the Aspen Plus simulation by specifying the yields in an RYIELD reactor. The solid residue consisting of unreacted char and ash rolls down the length of the sloped kiln and is discharged at the reactor outlet while the raw gas is first directed to a cyclone to remove any entrained ash or unconverted char, and then to a tar cracking unit to eliminate tars from the generated syngas [14]. The syngas is then cooled to 200 °C and passed through a ceramic barrier filter for removal of particulate matter before being directed to the acid gas removal section.

Similar to the experimental setup in [27], the gasifier is indirectly fired by housing the kiln in a furnace operating at 1050 °C as illustrated in [44]. The entire fuel requirement for the furnace is provided by the unreacted char

from the rotary kiln which is mixed with preheated air for combustion. In order to minimize heat loss and protect the shell of the furnace, a refractory lining is used on the inner side of the wall between the furnace and the ambient air. The wall between the furnace and the gasifier is made out of a temperature-resistant alloy in order to maximize heat transfer to the kiln [44]. The pyrolysis (breakdown) of the solid char to elemental species is first modeled as a decomposition process occurring at 500 °C in an RYIELD block together with a calculator block that specifies the component yields according to the ultimate composition of the char. Then the combustion reaction is modeled using the RGIBBS reactor assuming unrestricted chemical equilibrium to give flue gas and ash. The air flowrate is adjusted such that the heat requirement of the gasifier is satisified. Heat loss to the environment of 1% of the gasifier duty is assumed and included in the energy balance calculations.

2.2.2. Acid Gas Removal

The gaseous product contains 0.03 mol% COS that needs to be removed to sub-ppm levels to prevent poisoning of downstream catalysts. The COS hydrolysis process is used to convert COS to H_2S. This process is modeled with the REQUIL reactor in Aspen Plus assuming chemical equilibrium is achieved. In order to achieve 99.5% COS conversion, an activated alumina-based catalyst is used [45]. The syngas is then cooled and flashed before heading to the acid gas removal section. Physical absorption is used for removal of H_2S and CO_2 using MDEA as a solvent. The process detailed in [38] is used. The low pressure absorber is used to remove H_2S. The sweetened gas is then compressed to 23 bar for CO_2 removal and the captured sour gas stream is sent to the Claus section. Piperazine is added to the solvent in the CO_2 removal section to enhance absorption. It is essential to control the amount of CO_2 removed in the MDEA section because the conversion of syngas in the downstream methanation process is sensitive to the relative ratios of CO, CO_2, and H_2 [46]. The contribution of the CO_2 feed fraction to the methanation process through the Sabatier reaction is accounted for by using the "feed gas module", M, (Equation 1) which is set to 3 to maximize methane production [46]. This specification resulted in 87.8 wt % CO_2 removal from syngas.

$$M = \frac{X_{\mathrm{H_2},feed} - X_{\mathrm{CO_2},feed}}{X_{\mathrm{CO},feed} + X_{\mathrm{CO_2},feed}} \tag{1}$$

Simulation of the H_2S and CO_2 removal processes is done using BR&E's ProMax software as detailed in [38].

2.2.3. Claus process

The Claus process serves the dual purpose of treating the captured H_2S to prevent emissions to the outside air and producing elemental sulfur as a valuable by-product. The two key reactions that occur are the partial oxidation of H_2S to produce SO_2 (Equation 2), and the reaction of H_2S with the produced SO_2 to produce elemental sulfur (Equation 3).

$$H_2S + \frac{3}{2}\,O_2 \rightleftharpoons SO_2 + H_2O \tag{2}$$

$$2\,H_2S + SO_2 \rightleftharpoons 2\,H_2O + 3\,S \tag{3}$$

The relatively small quantity of oxygen required is assumed to be available on-site as a utility. Two stages of conversion to sulfur take place with intermediate sulfur condensation and removal in order to drive the forward reaction resulting in a sulfur recovery of 96% [40]. The unreacted H_2S after the second stage is recycled back to the MDEA H_2S removal process. The produced sulfur is cooled and stored for sale. A rigorous model is developed in Aspen Plus for the Claus process using the approach detailed in [47].

2.2.4. Methanation

The TREMP methanation process by Haldor-Topsøe was used, which consists of four catalytic fixed bed reactors each operating at a temperature of 300 °C with intermediate cooling [41], [46]. Hydrogenation of CO and CO_2 occurs over a nickel-based catalyst according to the methanation and Sabatier reactions, which are presented in Equations 4 and 5 respectively. Due to the highly exothermic nature of these two reactions, it is necessary to implement a temperature control strategy, such as recycling a substantial fraction of the product from the first reactor in order to dilute the feed, in addition to using high temperature tolerant catalysts. The outlet stream from the third reactor is cooled to 150 °C and condensed water removed so as to enhance the conversion to methane in the final reactor. The SNG product stream is passed through a molecular sieve in order to remove 98.5 vol% of CO_2 and any remaining water to sub-ppm levels. Molecular sieves are designed to separate molecules based on differences in polarity and molecular

size as detailed in [48]. The SNG product is then compressed to 55 bar in order to satisfy specifications for the natural gas liquefaction process [40].

$$\mathrm{CO} + 3\,\mathrm{H_2} \rightleftharpoons \mathrm{CH_4} + \mathrm{H_2O} \tag{4}$$

$$\mathrm{CO_2} + 4\,\mathrm{H_2} \rightleftharpoons \mathrm{CH_4} + 2\,\mathrm{H_2O} \tag{5}$$

2.2.5. Liquefaction of SNG

The pressurized SNG stream is desuperheated, liquefied, and subcooled in a multistream plate-and-fin type heat exchanger [31] before exiting as liquefied SNG at -157 °C. The cooling duty is provided by a refrigeration cycle. The refrigerant stream operates at two pressure levels, as shown in Figure 1: High pressure refrigerant is partially-liquefied in a condenser and then enters the multistream heat exchanger as a hot stream where it is also cooled to -157 °C before undergoing adiabatic expansion through a throttle valve. The expansion slightly lowers the stream temperature after which the low pressure refrigerant re-enters the multistream heat exchanger as the only cold stream. Vaporization of the low pressure refrigerant provides the entire refrigeration duty for the system. The evaporated refrigerant then undergoes two-stage compression with intercooling to complete the cycle.

Determining the optimal operating conditions for the liquefaction process is a subject of active research [49]. In this work, we used the operating conditions suggested by Watson et al. [31] (presented in Table 2) which show good agreement with the results of Austbø and Gundersen [50]. The results from the case with maximum heat exchanger conductance (UA_{max}) set to 25 MW/K were used.

Simulation of the natural gas liquefaction process is challenging particularly as a result of the complex multistream heat exchanger block. Simulation in Aspen Plus with the MHEATX block commonly fail to converge to a physical solution especially if done in isolation [51]. This is because the MHEATX block only solves an energy balance of the multistream heat exchanger but does not have constraints to prevent temperature crossovers, thus making it necessary to either know in advance which operating conditions and heat exchanger parameter values avoid crossovers or perform a "guess-and-check" procedure. To avoid these issues, in this work the values of all pressures and compositions (except for the outlet temperature of the low pressure refrigerant) obtained from an equation-based simulation done in a previous study [31], [51] are passed on to the MHEATX block. The MHEATX block

is discretized into 10 zones with the option to add extra zones for phase change, and stream entry/exit enabled. The MHEATX block then solves for the low pressure refrigerant outlet temperature, and provides results of the zone profiles, duties, UA value and log mean temperature difference. Thus, the Aspen Plus simulation is used to validate the physical feasibility of the operating conditions suggested in [31].

2.2.6. Heat Integration and Steam Generation

In order to minimize utility costs and increase energy efficiency, a heat integration strategy is implemented on a plantwide scale. Relevant stream data (supply and target temperatures, heat capacities, flowrates) are exported from the Aspen Plus and ProMax simulations to the commercial Aspen Energy Analyzer (AEA) software. Data on the available utilities are also specified in AEA; Cold utilities considered are Cooling water, LP, MP, and HP steam generation while hot utilities considered are LP, MP, and HP steam as detailed in Table 2.

AEA determines (near) optimal designs of the heat exchanger network (HEN) using a methodology detailed by Shethna et al. [52]. Default cost correlations are used for the heat exchangers. The Grand Composite Curve utility allocation method is used as a heuristic to maximize the use of the utilities closest to the pinch (the hottest cold utilities and the coldest hot utilities i.e. the cheapest utilities) first. Default values for the unit costs of utilities in Aspen Plus are used as detailed in Table 2, with steam generation incurring a negative cost. The cooling water system consists of an evaporative mechanical draft multicell cooling tower, circulating water pumps, and a make-up water system as detailed in [45]. AEA does not guarantee a globally optimal HEN design. Thus, in this work, the best design in terms of lowest TAC out of 100 proposed near-optimal designs is chosen. A visual representation of the HEN design is presented in the Excel sheets in the Supplementary Materials.

2.3. Case 2: With precombustion CCS

The case with precombustion CO_2 capture has essentially the same units as Case 1 except that the CO_2 captured in the MDEA unit goes through a two stage compression process with intercooling and water removal to supercritical conditions. The CO_2 is then pumped to 153 bar.

2.4. Case 3: With pre- and postcombustion CCS

The case with postcombustion CO_2 capture has essentially the same units as Case 2 except that an additional DGA-based unit is included to remove CO_2 from the flue gas exiting the furnace. The DGA process is similar to the MDEA process and is detailed in [38]. The captured CO_2 stream is directed to the CO_2 compression and liquefaction section prior to sequestration.

2.5. Economic Analysis

The three waste to liquefied SNG design strategies are compared using a profitability analysis for the two plant locations. The net present value (NPV) is calculated using the discounted cash flow rate of return approach. The approach follows the work of Seider et al. [53]. The base scale used for the economic analysis is 893 $MW_{LHV,input}$ (consistent with the analysis of Larson et al. [14]) equivalent to 26.3 kg/s of waste tire. All cases also have the same SNG output of 483.8 MW_{LHV}.

The capital costs of the different pieces of equipment are estimated from data available for similar processing units in established literature sources as presented in the Supplementary Materials. For sections where cost data is not available, we make conservative estimates based on the most similar unit operations available in the literature. For instance, the capital costs of the waste tire shredding plant is estimated from [39] with the conservative assumption that the cost to produce crumb tire of size 6 mm is one third of that to produce 0.18 mm. Similarly, for the rotary kiln gasifier, we effectively double the capital cost estimate (by using a process contingency of 100%) presented in [54] for the related use of rotary kilns in cement manufacture. For the indirect firing, we include the additional cost of a furnace using an estimate made using Aspen Process Economic Analyzer (APEA). Finally, the multistream heat exchanger in the liquefaction section is costed using the method outlined by Fu and Gundersen [55] using Equation 6

$$C_{MSHE} = f_m r_p C_{volume} V_{MSHE} \tag{6}$$

where C_{volume} [$\$_{2018}/m^3$] is the MSHE cost per unit volume and V_{MSHE} [m^3] is the volume of the MSHE. The factors f_m and r_p take on values of 2.0 and 1.1 and are used to account for the installation costs and MSHE operation at pressures higher than 25 bar respectively. The volumetric heat transfer coefficient method is used to determine C_{volume} following the methodology

outlined in [56]. The MSHE is divided into zones, and the volume corresponding to each zone (V_z) is calculated using Equation 7. A local volumetric heat transfer coefficient (β_z) of 100 kW/m^{3}K [57] is assumed while the zone duties ($\dot{Q}_z$) and zone LMTDs ($\Delta T_{m,z}$) are obtained using the MHEATX simulation in Aspen Plus.

$$V_z = \frac{\dot{Q}_z / \Delta T_{m,z}}{\beta_z} \tag{7}$$

The overall MSHE volume is determined using Equation 8 with an additional 15% allowance for headers.

$$V_{MSHE} = 1.15 \sum_{i=1}^{n} V_z \tag{8}$$

A C_{volume} of 20,800 [$\$_{1997}$/m^3] is assumed with the costs scaled to $\$_{2018}$ using the CEPCI index method [55].

Variable operating costs including raw material, catalyst and solvent, and waste disposal costs are estimated from closely related sections in published reports as detailed in the Supplementary Materials. For the base case, no cost or tipping fees are assumed for the waste tires and no CO_2 taxes are levied; the influence of these two factors on plant profitability is determined using a sensitivity analysis. Utility costs are estimated from AEA. The electricity requirement for preparation and shredding of waste tire (El_{tire}) [kWh/ton] is determined using the correlation with final crumb tire size (S_{tire} [inch]) suggested in [39] (Equation 9).

$$El_{tire} = 97.91 S_{tire}^{-0.222} \tag{9}$$

A capacity factor of 85 % is assumed. All costs are scaled to $\$_{2018}$ assuming a yearly inflation rate of 2.75 %. The fixed operating costs including labor, maintenance, operating overhead, and property insurance and tax costs are estimated based on the methodology of Seider et al. [53] as detailed in Supplementary Materials. A purchasing power parity (PPP) for Norway of 10.142 NOK/USD and an average exchange rate of 8.133 NOK/USD is used. The minimum selling price (MSP) of liquefied SNG is calculated as the value that results in a NPV of zero. For the base case, the assumed parameters for the discounted cash flow rate of return analysis to calculate the NPV are presented in the Supplementary Materials.

3. Results and Discussion

3.1. Simulation results

The Aspen Plus and ProMax simulation files are made open-source and are available for download at the LAPSE digital archive at:
http://psecommunity.org/LAPSE:2019.1261 [58].
In addition, the Excel sheets containing relevant stream conditions, CAPEX and OPEX calculations as well as the Discounted Cash Flow Rate of Return (DCFROR) analysis are made available.

3.1.1. Thermodynamic analysis

A summary of the power consumed by the various sections as well as plantwide utility requirements are presented in Table 4. The fuel efficiency (Equation 10) only considers the proportion of the feedstock that is converted to the final product and so neglects the energetic input in utilities and electricity. The contribution of utilities and electricity is accounted for in the overall energy efficiency (Equation 11).

$$\eta_{fuel} = \frac{SNG_{LHV}}{Tire_{LHV}} \tag{10}$$

$$\eta_{energy} = \frac{SNG_{LHV}}{Tire_{LHV} + Electicity\ consumed + Utilities\ consumed} \tag{11}$$

Only a small energy penalty is incurred by incorporating precombustion CCS (Case 2) because CO_2 has to be separated anyway in Case 1. However, including postcombustion CO_2 capture results in a substantially lower energy efficiency because the parasitic load of the DGA process is supplied by additional LP steam. Table 4 shows that it is possible to recover 54.2% of the energy content of waste tires as liquefied SNG. In addition, for each kg of waste tire converted, 0.37 kg of liquefied SNG is obtained thus illustrating the potential value of the concept.

No comparable research efforts exist for the production of SNG from waste tires. Instead, we provide a comparison with studies on biomass-based SNG production. Van der Meijden et al. reported overall energy efficiencies of $54\%_{LHV}$, $58\%_{LHV}$ and 67 $\%_{LHV}$ for entrained flow, circulating fluidized bed and indirect-fired gasification respectively [33]. Zwart et al. estimated an energy efficiency of 70% [34] while Gassner and Maréchal reported overall

efficiencies of 65-76 $\%_{LHV}$ [35], [36]. The lower efficiency of the proposed concept can be partly explained by the fact that biomass typically has a very low sulfur content (less than 0.1% [59]) thus separate H_2S removal using the energetically expensive MDEA and Claus processes is not necessary. Instead, the small quantities of H_2S can be co-removed with CO_2 and oxidized to SO_2 and released to the atmosphere at levels substantially below emission limits [14]. In addition, inefficiency arises from running the gasifier at atmospheric pressure which necessitates expensive syngas compression prior to CO_2 compression. Thus, there is substantial scope for optimization with different gasifier configurations, and these will be explored in future work. For instance, using entrained flow gasification (with essentially the same gasifier design used commercially for coal gasification) at higher temperatures and pressures may result in higher syngas yields and thus efficiencies as well as allow the use of different acid gas removal strategies like the selexol process. In addition, using entrained flow gasification with hybrid feedstocks has been shown to increase efficiency as a result of tighter heat integration of the high temperature syngas cooling section with endothermic processes such as natural gas reforming [15], [16], .

3.1.2. CO_2 emissions

The carbon efficiency of the three design configurations which denotes the percentage of carbon atoms in the waste tires that end up in the liquefied SNG is calculated using Equation 12.

$$\eta_{carbon} = \frac{SNG_{carbon}}{Tire_{carbon}} \tag{12}$$

The direct and indirect emissions associated with the waste tire to liquefied SNG concept for the three design cases and two locations are presented in Table 5. The direct emissions include all the GHG emissions (converted to equivalent CO_2 emissions) from processes occurring within the plant gates while the indirect emissions include all the supply chain emissions associated with all the process inputs such as electricity and utilities which vary with location. The GHG emissions computed followed the International Panel on Climate Change (IPCC) 100-year metric. However, indirect emissions involved in the manufacture of process equipment are not included; performing a full life cycle analysis of the process is left as future work. Electricity emissions are estimated based on statistics for the average electricity mix in 2017 of 687.5 $kg_{CO_2,eq}$/MWh [60] and 16.4 $kg_{CO_2,eq}$/MWh [61] for the US and

Norway respectively. The indirect emission factors of utilities are determined with data from the EPA [62]: Steam & heat, and cooling water have emissions of 0.128 $kg_{CO_2,eq}$/MJ and 0.016 $kg_{CO_2,eq}$/MJ respectively [63]. Indirect emissions for waste tires are assumed to be zero; emissions associated with tire manufacturing are attributed to the automobile sector. The emissions that may arise out of stockpiling tires are not considered as well.

Indirect emissions are highest for Case 3 with postcombustion CO_2 capture as a result of higher steam requirements for the DGA process as well as higher electricity for CO_2 compression and liquefaction. Total GHG emissions are substantially lower for the cases with CO_2 capture. In order to quantify the economic penalty of implementing pre- or postcombustion CO_2 capture, we calculate the cost of CO_2 capture (CCC) metric (defined according to Equation 13). The results (presented in Table 5) show that implementing only pre-combustion CCS results is substantially cheaper than implementing both pre- and postcombustion CCS since CO_2 has to be separated prior to methanation whether CCS is implemented or not.

$$CCC = \frac{MSP_{Design\ with\ CCS} - MSP_{Design\ without\ CCS}}{GHG_{Design\ without\ CCS} - GHG_{Design\ with\ CCS}} \tag{13}$$

In order to quantify the relative environmental performance of the proposed process, we compare the total emissions with those associated with the status quo (conventional natural gas). For this study, we used 20 $kg_{CO_2,eq}/GJ_{LHV}$ as the value of total emissions associated with extraction and transportation of conventional natural gas [64]. Factoring this into account, only the case with both pre- and postcombustion CO_2 capture implemented in Norway has a net reduction in life cycle global warming potential compared to conventional natural gas. For this case, we calculate the cost of CO_2 avoided (CCA) using Equation 14 to be 1,313 $\$/tonne_{CO_2,eq}$. While this is expensive, similarly high CCA values are attained for the production of biological biobutanol (472 $\$/tonne_{CO_2,eq}$) [65], thermochemical biobutanol (136 $\$/tonne_{CO_2,eq}$) [66], biodiesel (400 $\$/tonne_{CO_2,eq}$) [67], or corn ethanol (potentially up to 750 $\$/tonne_{CO_2,eq}$) [17], [67]. We note that since the majority of emissions arise as indirect emissions from the high electricity requirement (primarily required for syngas compression prior to CO_2 removal), a potential option to improve environmental performance is to use a different gasifier configuration with higher operating pressure.

$$CCA = \frac{MSP_{SNG\ plant} - MSP_{conventional\ NG}}{GHG_{conventional\ NG} - GHG_{SNG\ plant}} \tag{14}$$

Case		Case 1	Case 2	Case 3
CCS enabled?		No	Only precombustion	Both pre- & postcombustion
Waste tire flow rate	kg/s	26.3	26.3	26.3
Thermal input	MW_{LHV}	893	893	893
Total electricity requirement	MW	59.62	61.71	63.84
Grinding to crumb tire	MW	14.1	14.1	14.1
Syngas compression	MW	32.9	32.9	32.9
H_2S stream compression	MW	0.1	0.1	0.1
Methanation recycle compression	MW	0.3	0.3	0.3
MDEA pump	MW	0.5	0.5	0.5
SNG compression	MW	2.1	2.1	2.1
Liquefaction compressor duty	MW	9.7	9.7	9.7
CO_2 compressor duty	MW	0.0	2.1	4.2
Net hot utility requirement	MW	157.7	159.1	283.9
LP steam	MW	-16.1	-16.0	-16.0
MP steam	MW	173.8	175.1	299.9
HP steam	MW	<0.1	<0.1	<0.1
Total cooling water requirement	MW	535.2	540.7	622.5
SNG flowrate	kg/s	9.7	9.7	9.7
Sulfur flowrate	kg/s	0.3	0.3	0.3
Heating value of SNG produced	MW_{LHV}	483.8	483.8	483.8
Heating value of SNG produced	MW_{HHV}	537.5	537.5	537.5
Overall Fuel Efficiency (η_{fuel})	$\%_{LHV}$	54.2	54.2	54.2
Overall Fuel Efficiency (η_{fuel})	$\%_{HHV}$	55.7	55.7	55.7
Overall Energy Efficiency (η_{energy})	$\%_{LHV}$	43.6	43.4	39.0
Overall Energy Efficiency (η_{energy})	$\%_{HHV}$	45.4	45.3	40.9

Table 4: Energy balances for the three designs. These energy balances are independent of location.

Case		Case 1	Case 1	Case 2	Case 2	Case 3	Case 3
Location		USA	Norway	USA	Norway	USA	Norway
CCS enabled?		No	No	Only precombustion	Only precombustion	Both pre- & post combustion	Both pre- & postcombustion
Direct GHG emitted	$Mt_{CO_2,eq}$/year	1.19	1.19	0.62	0.62	0.03	0.03
CO_2 sequestered	Mt/year	0.00	0.00	0.57	0.57	1.16	1.16
Indirect GHG emitted	$Mt_{CO_2,eq}$/year	0.57	0.01	0.59	0.01	0.81	0.02
Total GHG emitted	$Mts_{CO_2,eq}$/year	1.76	1.20	1.20	0.63	0.84	0.05
Direct GHG emitted (scaled)	$kg_{CO_2,eq}/GJ_{SNG}$	91.69	91.69	47.57	47.57	2.38	2.38
Indirect GHG emitted (scaled)	$kg_{CO_2,eq}/GJ_{SNG}$	44.07	1.05	45.07	1.08	62.17	1.48
Total GHG emitted (scaled)	$kg_{CO_2,eq}/GJ_{SNG}$	135.75	92.74	92.64	48.65	64.55	3.86
Carbon efficiency	%	35.7	35.7	35.7	35.7	35.7	35.7
CCS	$\$/t_{CO_2,eq}$	-	-	18.6	20.4	44.9	45.0
CCA	$\$/t_{CO_2,eq}$	-	-	-	-	-	1,313

Table 5: Environmental performance of three design strategies for the two locations.

Case		Case 1	Case 1	Case 2	Case 2	Case 3	Case 3
Location		USA	Norway	USA	Norway	USA	Norway
CCS enabled?		No	No	Only precombustion	Only precombustion	Both pre- & post combustion	Both pre- & postcombustion
Total capital costs	M$	746.3	930.7	751.6	937.3	825.2	1,029.1
Solids handling	M$	48.8	60.8	48.8	60.8	48.8	60.8
Crumb rubber plant	M$	30.3	37.8	30.3	37.8	30.3	37.8
Water systems	M$	103.0	128.4	103.7	129.4	114.5	142.8
Ash cyclone, tar cracker & ceramic filter	M$	84.9	105.9	84.9	105.9	84.9	105.9
Rotary kiln gasifier & Furnace	M$	77.1	96.2	77.1	96.2	77.1	96.2
Gas cleaning	M$	144.9	180.7	144.9	180.7	198.7	247.7
Syngas compression	M$	58.8	73.4	58.8	73.4	58.8	73.4
Claus process	M$	18.2	22.7	18.2	22.7	18.2	22.7
Methanation	M$	33.1	41.2	33.1	41.2	33.1	41.2
SNG purification & compression	M$	20.4	25.4	20.4	25.4	20.4	25.4
CO_2 compression	M$	0.0	0.0	3.9	4.8	7.8	9.7
SNG liquefaction	M$	20.5	25.6	20.5	25.6	20.5	25.6
Heat Exchanger Network	M$	3.1	4.0	3.5	4.4	3.8	4.7
Miscellaneous	M$	52.6	65.6	52.6	65.6	52.6	65.6
Initial catalyst and solvent fill	M$	1.7	2.1	1.7	2.1	1.9	2.3
Land	M$	13.9	17.4	14.1	17.5	15.4	19.2
Working capital	M$	34.9	43.5	35.1	43.8	38.6	48.1
Total annual costs (85% capacity)	M$/yr	125.2	156.2	134.1	167.2	161.6	201.6
Raw materials, Solvents & Catalysts	M$/yr	1.1	1.4	1.1	1.4	1.2	1.5
Waste disposal	M$/yr	1.9	2.4	1.9	2.4	1.9	2.4
Utilities & HEN operating costs	M$/yr	45.0	56.2	46.3	57.7	54.7	68.2
Total labor costs	M$/yr	13.0	16.3	13.0	16.3	13.8	17.3
Maintenance	M$/yr	44.9	56.0	45.2	56.4	49.7	61.9
Operating overhead	M$/yr	8.2	10.3	8.3	10.3	9.0	11.3
Property insurance & tax	M$/yr	11.1	13.9	11.2	14.0	12.4	15.4
Minimum Selling Price	$/GJ$_{LHV}$	16.7	20.9	17.5	21.8	19.9	24.9

Table 6: Summary of economic analysis of the three design strategies for the two locations

3.1.3. Economic Analysis

The results of the economic analysis for the different case studies are summarized in Table 6 with further details on the capital costs, annual operating costs and the discounted cash flow rate of return analysis available in the Supplementary Material. Cases 1, 2, and 3 have minimum selling prices for liquefied SNG of 16.7, 17.5 and 19.9 \$/GJ_{LHV} in the US and 20.9, 21.8 and 24.9 \$/GJ_{LHV} in Norway. All these prices are higher than the prices of conventional LNG in most locations which range from 2.90 \$/GJ_{LHV} to 9.85 \$/GJ_{LHV} [68]. This implies that the proposed concept is not profitable at current market conditions.

However, the minimum selling prices are comparable to those from SNG production from biomass. For instance, Batidzirai et al. report prices of 18.6 to 25.9 \$/GJ_{LHV} for the 100 MW (thermal input) scale, and prices of 12.6 to 17.4 \$/GJ_{LHV} at the 1000 MW (thermal input) scale although this value includes supply chain costs such as LNG transportation, regasification, compression and delivery to refuelling stations [32]. The minimum selling prices are lower than the range of 23.45 \$/GJ_{LHV} (76 €/MWh) to 33.02 \$/GJ_{LHV} (107 €/MWh) for the 20 MW (thermal input) scale and 18.20 \$/GJ_{LHV} (59 €/MWh) to 29.93 \$/GJ_{LHV} (97 €/MWh) for the 150 MW (thermal input) scale reported by Gassner and Marechal [35]. Zwart et al. report total SNG production costs of 34.22 \$/GJ_{LHV} at the 10 MW (thermal input) scale and 17.00 \$/GJ_{LHV} at the 100 MW (thermal input) scale [34].

We also note that the proposed process designs may become competitive under certain regulatory conditions. For instance, there is public policy movement in British Columbia (Canada) that requires public utilities to purchase natural gas made from renewables at prices up to 30\$/GJ_{LHV} [69]. In addition, the minimum selling prices are competitive with oil prices. A historical plot between 1984 and 2018 of the inflation-adjusted prices of natural gas and oil is available in our previous work [70]; oil prices ranged from 3 \$/GJ in 1999 to 24 \$/GJ during the energy crisis in 2008, with a recent price (June 2018) of 10.3 \$/GJ [71]. The impact of plant scale, waste tire tipping fees and CO_2 taxes on minimum selling prices, and of liquefied SNG prices on net present value (NPV) are presented in the sensitivity analysis section.

3.2. Sensitivity Analysis

The results presented in the previous section are based on an assumed set of economic parameters which vary significantly over time and in different

locations worldwide. In order to determine the impact on economic performance as a result of different realizations of these uncertain parameters, a sensitivity analysis was performed. Figure 2 shows the impact of the Liquefied SNG price on NPV, with the minimum selling price resulting in an NPV of 0 $.

Figure 3 shows the impact of the plant scale on the MSP of liquefied SNG. The results show that economies of scale have a substantial impact on lowering the MSP with large reductions in cost occurring for plant scales to 1000 MW (thermal input). However, we note that 100 MW of waste tire thermal input corresponds to approximately 10.5 million tires per year thus larger plant scales may necessitate either importing waste tires (for the Norwegian case) or situating the plant in a location with a high population density. One promising alternative that will be investigated in future work that retains the benefits of economies of scale is to utilize additional feedstocks such as waste plastics, municipal solid waste or natural gas.

Figure 4 shows that tipping fees of waste tires has a substantial impact on the MSP. Typical waste tire fees are in the range of 35 - 150 $/tonne [39], with Sweden having a higher landfilling tax of 193 $/tonne [72]. The results show that the proposed concept would become cost competitive with natural gas (at the upper price range of 9.85 $/GJ$_{LHV}$) if tipping fees are increased to higher than 140 $/tonne in the USA.

Figure 5 shows that for all cases, levying CO_2 taxes increases the minimum selling price since the plant has positive direct emissions. However, the MSP for the cases with CO_2 capture enabled increases to a smaller extent. Enabling pre-combustion CCS becomes the cheapest option at tax rates higher than 20 $/tonne$_{CO_2}$ while postcombustion CCS becomes cheapest at tax rates higher than 54 $/tonne$_{CO_2}$ in both locations.

Figure 6 quantifies the relative impact of various process and economic parameters on the minimum selling price of SNG for Case 1 (USA). The key process parameters studied were the gasifier yield and the overall conversion in the methanation unit. In order to give a conservative estimate, the gasifier yield was adjusted to be 90% and 80% of the base case which resulted in an increase in the MSP of SNG of +8.9% and +14.0% respectively. Similarly, the overall conversion in the methanation section was adjusted to be 0.90 and 0.85 which resulted in an increase in SNG MSP of +8.4% and 14.5%. Various economic parameters such as Internal Rate of Return (IRR), Inflation %, Plant lifetime, Working Capital %, Loan Interest Rate, On stream %, Waste tire tipping fees, and Plant Scale were also studied. Waste tire tipping fees

are shown to have the greatest impact on the MSP (with 50.0 $/tonne and 100.0 $/tonne resulting in lower MSPs by -16.2% and -32.5%. Similarly, the plant scale has a substantial impact: An increase in scale by approximately one third (to 1200 MW) results in a lower MSP by 8.6% while a decrease in scale by approximately one third (to 600 MW) results in a higher MSP by 13.7%. The on-stream % and IRR are shown to have a sizeable impact on the MSP as well. Comparing the relative impact of the different parameters presented in Figure 6, we note that although process parameters have a sizeable impact on the MSP, certain economic parameters such as plant scale and waste tire tipping fees have an even larger impact and these are further studied in Figure 4 and 3 respectively.

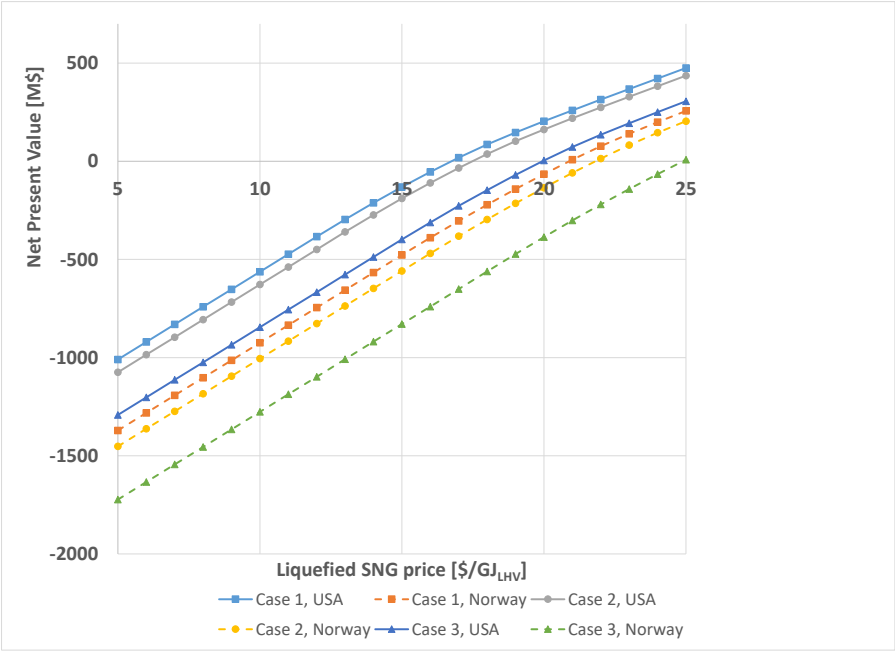

Figure 2: Impact of liquefied SNG prices on Net Present Value

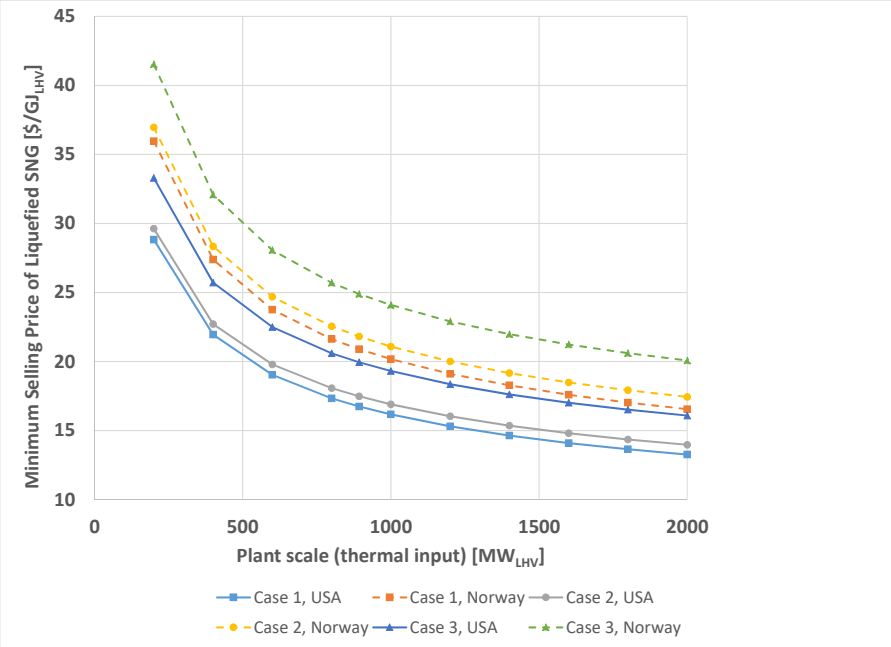

Figure 3: Impact of plant scale (thermal input) on the SNG minimum selling price

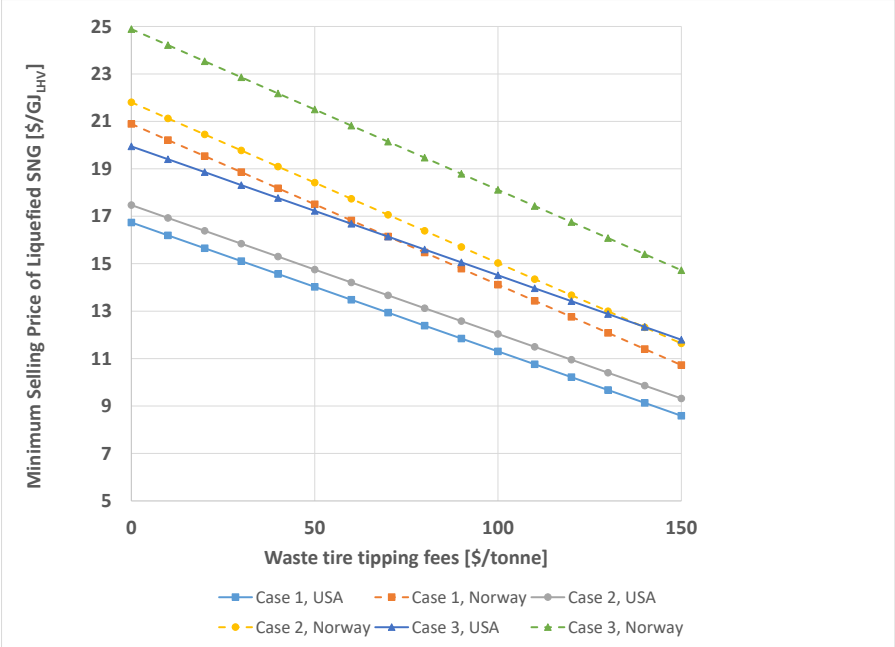

Figure 4: Impact of waste tire tipping fees on the SNG minimum selling price

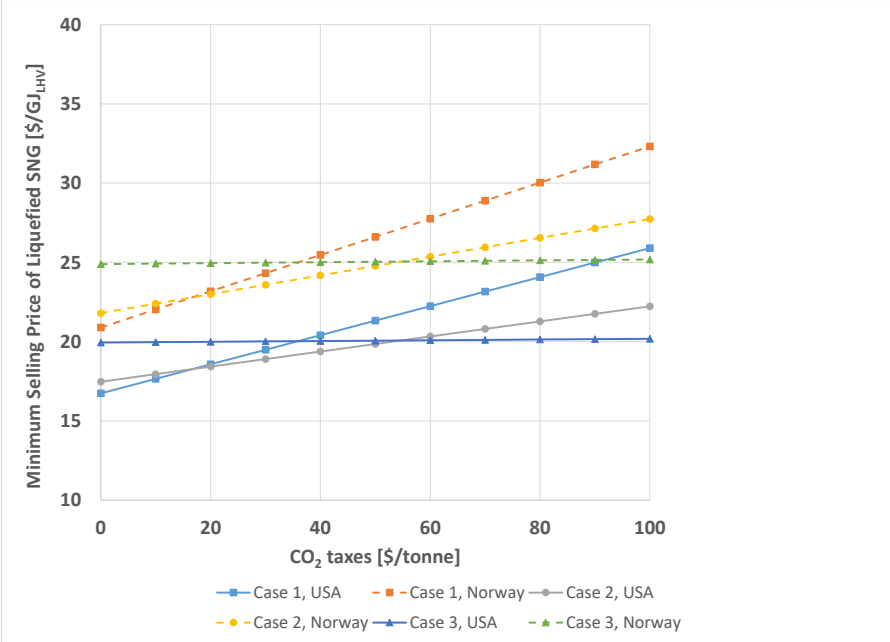

Figure 5: Impact of CO_2 taxes on the SNG minimum selling price

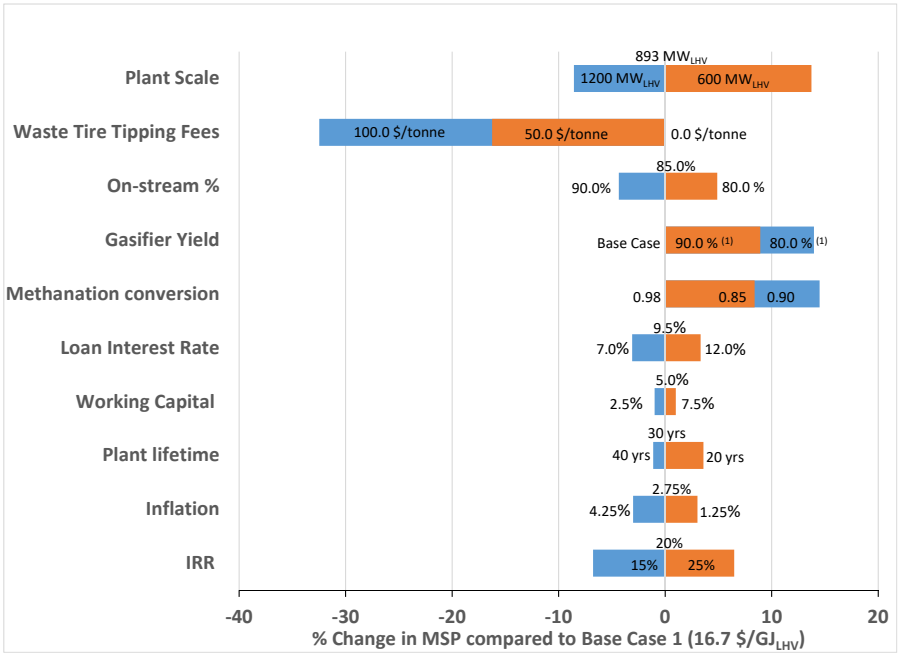

Figure 6: Tornado Plot to show the relative impact of changing certain economic and process parameters on the SNG minimum selling price for Case 1 - USA. [1] Sensitivity analysis is performed by considering cases with 90.0% and 80.0% of the base case gasifier yield. IRR denotes the Internal Rate of Return.

4. Conclusions and Future work

The proposed waste to liquefied SNG concept was found to be technologically feasible. Results of the energy analysis showed that the concept was less efficient than comparable biomass to SNG processes mostly because of the need for energetically expensive sulfur removal processes. The design situated in Norway for which both pre- and postcombustion CO_2 capture is implemented was found to be environmentally favorable to conventional natural gas extraction as it had near zero direct and indirect CO_2 emissions. Other designs may become competitive with conventional natural gas extraction under certain regulatory conditions. In addition, the minimum selling prices were found to lie within the range of oil prices in the recent decade. We also found that the minimum selling price reduces substantially with process scale and levying tipping fees. While various uncertain process parameters such as the gasifier yield and overall conversion of the methanation section have a sizeable impact on the MSP, the influence of plant scale and waste tire tipping fees is larger.

Significant avenues for investigation and process improvement exist and these will be addressed in future work. First, different gasifier configurations such as high temperature and pressure entrained flow gasification with multiple feedstocks can be studied. In addition, different product portfolios can be investigated including production of multiple products as part of a polygeneration scheme. The design of flexible processes that are able to handle significant exogeneous uncertainties in market prices and CO_2 taxes can also be investigated.

Acknowledgements

The first author gratefully acknowledges the financial support of the Ph.D. scholarship from NTNU's Department of Energy and Process Engineering. We thank Ikenna J. Okeke of McMaster University for helpful discussions.

Conflicts of Interest

The authors declare no conflicts of interest.

Nomenclature

β_z Local volumetric heat transfer coefficient

$\Delta T_{m,z}$ LMTD of zone z

ΔT_{min} Minimum temperature difference

$\dot{Q}_z$ Duty of zone z

η_{carbon} Carbon Efficiency

η_{energy} Energy Efficiency

η_{fuel} Fuel Efficiency

C_{MSHE} Cost of MSHE

CCA Cost of CO_2 Avoided

CCC Cost of CO_2 Capture

El_{tire} Electricity to shred tire

f_m MSHE Installation Cost factor

M Feed Gas module

r_p MSHE pressure factor

S_{tire} Final crumb tire size

V_z Volume of zone z of MSHE

AEA Aspen Energy Analyzer

APEA Aspen Process Economic Analyzer

C_{volume} MSHE cost per unit volume

CCS CO_2 Capture and Sequestration

DCFROR Discounted Cash Flow Rate of Return

DGA Diglycolamine

DME Dimethyl Ether

EF Entrained Flow (gasifier)

ElecNRTL Electrolyte Non-Random Two-Liquid equation of state

EPA US Environmental Protection Agency

GHG Greenhouse Gases

HRSG Heat Recovery Steam Generator

IPCC International Panel on Climate Change

IRR Internal Rate of Return

LAPSE Living Archive of Process Systems Engineering

LHV Lower Heating Value

LMTD Log mean temperature difference

LNG Liquefied Natural Gas

MDEA Methyldiethanolamine

MSHE Multistream Heat Exchanger

MSP Minimum Selling Price

NOK Norwegian Krone

NPV Net Present Value

PPP Purchasing Power Parity

PR-BM Peng-Robinson equation of state with the Boston-Mathias modification

PRICO Poly-Refrigerated Integrated Cycle Operations

SMR Single Mixed Refrigerant

SNG Synthetic Natural Gas

TREMP Topsøe Recycle Energy-efficient Methanation Process

UA_{max} Maximum heat exchanger conductance

V_{MSHE} volume of the MSHE

References

[1] V. Belgiorno, G. De Feo, C. Della Rocca, R. Napoli, Energy from gasification of solid wastes, Waste management 23 (2003) 1–15.

[2] J. D. Martínez, N. Puy, R. Murillo, T. García, M. V. Navarro, A. M. Mastral, Waste tyre pyrolysis–a review, Renewable and Sustainable Energy Reviews 23 (2013) 179–213.

[3] C. Peace, G. Petersen, M. Leary, P. Wiggins, Technology Evaluation and Economic Analysis of Waste Tire Pyrolysis, Gasification, and Liquefaction, Integrated Waste Management Board (2006).

[4] M. Labaki, M. Jeguirim, Thermochemical conversion of waste tyres—a review, Environmental Science and Pollution Research 24 (2017) 9962–9992.

[5] B. O. Oboirien, B. C. North, A review of waste tyre gasification, Journal of environmental chemical engineering 5 (2017) 5169–5178.

[6] Review of Technologies for Gasification of Biomass and Wastes, E4tech. http://www.e4tech.com/reports/review-of-technologies-for-gasification-of-biomass-and-wastes (2009).

[7] I. F. Elbaba, C. Wu, P. T. Williams, Hydrogen production from the pyrolysis–gasification of waste tyres with a nickel/cerium catalyst, International Journal of Hydrogen Energy 36 (2011) 6628–6637.

[8] I. F. Elbaba, P. T. Williams, Two stage pyrolysis-catalytic gasification of waste tyres: Influence of process parameters, Applied Catalysis B: Environmental 125 (2012) 136–143.

[9] I. F. Elbaba, P. T. Williams, High yield hydrogen from the pyrolysis–catalytic gasification of waste tyres with a nickel/dolomite catalyst, Fuel 106 (2013) 528–536.

[10] H. Karatas, H. Olgun, B. Engin, F. Akgun, Experimental results of gasification of waste tire with air in a bubbling fluidized bed gasifier, Fuel 105 (2013) 566–571.

[11] H. Karatas, H. Olgun, F. Akgun, Experimental results of gasification of waste tire with air&CO2, air&steam and steam in a bubbling fluidized bed gasifier, Fuel processing technology 102 (2012) 166–174.

[12] C. Wang, D. Leung, Characteristics of tyre powder gasification using a fluidized bed with an air/steam mixture, Sustainable Energy And Environmental Technologies (2001) 247–251.

[13] D. Leung, C. Wang, Fluidized-bed gasification of waste tire powders, Fuel Processing Technology 84 (2003) 175–196.

[14] E. D. Larson, H. Jin, F. E. Celik, Large-scale gasification-based coproduction of fuels and electricity from switchgrass, Biofuels, Bioproducts and Biorefining 3 (2009) 174–194.

[15] J. H. Ghouse, D. Seepersad, T. A. Adams II, Modelling, simulation and design of an integrated radiant syngas cooler and steam methane reformer for use with coal gasification, Fuel Processing Technology 138 (2015) 378–389.

[16] T. A. Adams II, P. I. Barton, Combining coal gasification and natural gas reforming for efficient polygeneration, Fuel Processing Technology 92 (2011) 639–655.

[17] I. J. Okeke, T. A. Adams II, Combining petroleum coke and natural gas for efficient liquid fuels production, Energy 163 (2018) 426–442.

[18] J. A. Scott, T. A. Adams II, Biomass-gas-and-nuclear-to-liquids (BGNTL) processes part I: Model development and simulation, The Canadian Journal of Chemical Engineering 96 (2018) 1853–1871.

[19] H. Boerrigter, A. Van Der Drift, Biosyngas: Description of R&D trajectory necessary to reach large-scale implementation of renewable syngas from biomass, Energy research Centre of the Netherlands (2004).

[20] A. S. R. Subramanian, T. Gundersen, T. A. Adams II, Optimal design and operation of a waste tire feedstock energy polygeneration system, In preparation (2020).

[21] A. S. R. Subramanian, T. A. Adams II, P. I. Barton, T. Gundersen, Optimal design and operation of a hybrid natural gas and waste tire feedstock energy polygeneration system, In preparation (2020).

[22] A. S. R. Subramanian, T. A. Adams II, T. Gundersen, P. I. Barton, Optimal design and operation of flexible polygeneration systems using decomposition algorithms, Computer-Aided Chemical Engineering (Accepted for ESCAPE 2020 - Milan, Italy) (2020).

[23] A. S. R. Subramanian, T. A. Adams II, T. Gundersen, P. I. Barton, Optimal design and operation of a hybrid natural gas and waste tire feedstock flexible polygeneration system using decomposition algorithms, In preparation (2020).

[24] U. Arena, Process and technological aspects of municipal solid waste gasification. A review, Waste management 32 (2012) 625–639.

[25] P. A. Amodeo, D. M. Goodale, D. J. Waage, R. F. Rynk, R. Comly, Alternative Energy Derived from Agricultural and Cafeteria Wastes using a Rotary Kiln Gasifier, in: American Society of Agricultural and Biological Engineers, p. 10.

[26] A. Donatelli, P. Iovane, A. Molino, High energy syngas production by waste tyres steam gasification in a rotary kiln pilot plant. Experimental and numerical investigations, Fuel 89 (2010) 2721–2728.

[27] S. Portofino, A. Donatelli, P. Iovane, C. Innella, R. Civita, M. Martino, D. A. Matera, A. Russo, G. Cornacchia, S. Galvagno, Steam gasification of waste tyre: Influence of process temperature on yield and product composition, Waste management 33 (2013) 672–678.

[28] T. A. Adams II, J. H. Ghouse, Polygeneration of fuels and chemicals, Current Opinion in Chemical Engineering 10 (2015) 87–93.

[29] S. Rönsch, J. Schneider, S. Matthischke, M. Schlüter, M. Götz, J. Lefebvre, P. Prabhakaran, S. Bajohr, Review on methanation–from fundamentals to current projects, Fuel 166 (2016) 276–296.

[30] Shell LNG Outlook, `https://www.shell.com/energy-and-innovation/natural-gas/liquefied-natural-gas-lng/lng-outlook-2019.html`, 2019. [Online; accessed 31-July-2019].

[31] H. A. Watson, M. Vikse, T. Gundersen, P. I. Barton, Optimization of single mixed-refrigerant natural gas liquefaction processes described by nondifferentiable models, Energy 150 (2018) 860–876.

[32] B. Batidzirai, G. S. Schotman, M. W. van der Spek, M. Junginger, A. P. Faaij, Techno-economic performance of sustainable international bio-SNG production and supply chains on short and longer term, Biofuels, Bioproducts and Biorefining 13 (2019) 325–357.

[33] C. M. van der Meijden, H. J. Veringa, L. P. Rabou, The production of synthetic natural gas (SNG): A comparison of three wood gasification systems for energy balance and overall efficiency, Biomass and bioenergy 34 (2010) 302–311.

[34] R. Zwart, H. Boerrigter, E. Deurwaarder, C. Van der Meijden, S. Van Paasen, Production of Synthetic Natural Gas (SNG) from biomass; development and operation of an integrated bio-SNG system; non-confidential version, Energy research Center of the Netherlands, Petten (2006).

[35] M. Gassner, F. Maréchal, Thermo-economic process model for thermochemical production of Synthetic Natural Gas (SNG) from lignocellulosic biomass, Biomass and bioenergy 33 (2009) 1587–1604.

[36] M. Gassner, F. Maréchal, Thermo-economic optimisation of the polygeneration of synthetic natural gas (SNG), power and heat from lignocellulosic biomass by gasification and methanation, Energy & Environmental Science 5 (2012) 5768–5789.

[37] H. Er-Rbib, C. Bouallou, Modeling and simulation of CO methanation process for renewable electricity storage, Energy 75 (2014) 81–88.

[38] T. A. Adams II, Y. K. Salkuyeh, J. Nease, Processes and simulations for solvent-based CO2 capture and syngas cleanup, in: Reactor and process design in sustainable energy technology, Elsevier, 2014, pp. 163–231.

[39] N. Sunthonpagasit, M. R. Duffey, Scrap tires to crumb rubber: feasibility analysis for processing facilities, Resources, Conservation and recycling 40 (2004) 281–299.

[40] R. Brasington, J. Haslbeck, N. Kuehn, E. Lewis, L. Pinkerton, M. Turner, E. Varghese, M. Woods, Cost and Performance Baseline for Fossil Energy Plants — Volume 2: Coal to Synthetic Natural Gas and Ammonia, Technical Report, DOE/NETL-2010/1402, 2011.

[41] N. Kezibri, C. Bouallou, Conceptual design and modelling of an industrial scale power to gas-oxy-combustion power plant, International Journal of Hydrogen Energy 42 (2017) 19411–19419.

[42] J. Klara, M. Woods, P. Capicotto, J. Haslbeck, N. Kuehn, M. Matuszewski, L. Pinkerton, M. Rutkowski, R. Schoff, V. Vaysman, Cost and performance baseline for fossil energy plants volume 1: Bituminous coal and natural gas to electricity. National Energy Technology Laboratory, Research and Development Solutions, LLC (RDS) (2007).

[43] S. Galvagno, G. Casciaro, S. Casu, M. Martino, C. Mingazzini, A. Russo, S. Portofino, Steam gasification of tyre waste, poplar, and refuse-derived fuel: A comparative analysis, Waste management 29 (2009) 678–689.

[44] The Rotary Kiln Handbook. FEECO International., `http://go.feeco.com/acton/media/12345/rotary-kiln-design`, 2019. [Online; accessed 02-August-2019].

[45] M. C. Woods, P. Capicotto, J. L. Haslbeck, N. J. Kuehn, M. Matuszewski, L. L. Pinkerton, M. D. Rutkowski, R. L. Schoff, V. Vaysman, Cost and performance baseline for fossil energy plants, National Energy Technology Laboratory (2007).

[46] J. Jensen, J. Poulsen, N. Andersen, From coal to clean energy, Nitrogen+ syngas 310 (2011) 34–38.

[47] R. P. Field, R. Brasington, Baseline flowsheet model for IGCC with carbon capture, Industrial & Engineering Chemistry Research 50 (2011) 11306–11312.

[48] Z. Y. Yeo, T. L. Chew, P. W. Zhu, A. R. Mohamed, S.-P. Chai, Conventional processes and membrane technology for carbon dioxide removal from natural gas: A review, Journal of Natural Gas Chemistry 21 (2012) 282–298.

[49] B. Austbø, S. W. Løvseth, T. Gundersen, Annotated bibliography — use of optimization in lng process design and operation, Computers & Chemical Engineering 71 (2014) 391–414.

[50] B. Austbø, T. Gundersen, Optimal distribution of temperature driving forces in low-temperature heat transfer, AIChE Journal 61 (2015) 2447–2455.

[51] M. Vikse, H. A. Watson, T. Gundersen, P. I. Barton, Versatile simulation method for complex single mixed refrigerant natural gas liquefaction processes, Industrial & Engineering Chemistry Research 57 (2017) 5881–5894.

[52] H. K. Shethna, J. Jezowski, F. Castillo, A new methodology for simultaneous optimization of capital and operating cost targets in heat exchanger network design, Applied Thermal Engineering 20 (2000) 1577–1587.

[53] W. D. Seider, J. D. Seader, D. R. Lewin, Product & Process Design Principles: Synthesis, Analysis and Evaluation, John Wiley & Sons, 2009.

[54] D. Barker, D. Holmes, J. Hunt, P. Napier-Moore, S. Turner, M. Clark, CO2 capture in the cement industry, Technical Report, 2008.

[55] C. Fu, T. Gundersen, Techno-economic analysis of CO2 conditioning processes in a coal based oxy-combustion power plant, International journal of greenhouse gas control 9 (2012) 419–427.

[56] G. F. Hewitt, S. J. Pugh, Approximate design and costing methods for heat exchangers, Heat transfer engineering 28 (2007) 76–86.

[57] ESDU, Selection and Costing of Heat Exchangers: Plate-Fin Type, ESDU Data Items (2003).

[58] Living Archive for Process Systems Engineering (LAPSE), `http://psecommunity.org/LAPSE:2019.1261`, 2019. [Online; accessed 02-August-2019].

[59] H. Jin, E. D. Larson, F. E. Celik, Performance and cost analysis of future, commercially mature gasification-based electric power generation

from switchgrass, Biofuels, Bioproducts and Biorefining 3 (2009) 142–173.

[60] U.S. Energy Information Administration. United States Electricity Profile 2017, https://www.eia.gov/electricity/state/unitedstates/, 2019. [Online; accessed 31-July-2019].

[61] Electricity disclosure 2017, https://www.nve.no/energy-market-and-regulation/retail-market/electricity-disclosure-2017/, 2017. [Online; accessed 02-August-2019].

[62] U.S. Environmental Protection Agency. Emission Factors for greenhouse gas inventories, https://www.epa.gov/sites/production/files/2018-03/documents/emission-factors_mar_2018_0.pdf, 2019. [Online; accessed 31-July-2019].

[63] Energy Star Portfolio Manager. Greenhouse Gas Emissions, https://portfoliomanager.energystar.gov/pdf/reference/Emissions.pdf, 2018. [Online; accessed 31-July-2019].

[64] Congressional Research Service. Canadian Oil Sands: Life-Cycle Assessments of Greenhouse Gas Emissions, https://fas.org/sgp/crs/misc/R42537.pdf, 2014. [Online; accessed 31-July-2019].

[65] G. Dalle Ave, T. A. Adams II, Techno-economic comparison of Acetone-Butanol-Ethanol fermentation using various extractants, Energy conversion and management 156 (2018) 288–300.

[66] C. O. Okoli, T. A. Adams II, Design and assessment of advanced thermochemical plants for second generation biobutanol production considering mixed alcohols synthesis kinetics, Industrial & Engineering Chemistry Research 56 (2017) 1543–1558.

[67] CBO. Using biofuel tax credits to achieve energy and environmental policy goals. In: Congress of the United States congressional budget office, https://www.cbo.gov/sites/default/files/111th-congress-2009-2010/reports/07-14-biofuels.pdf., 2010. [Online; accessed 3-December-2019].

[68] U.S. Energy Information Administration. U.S. Natural Gas Exports and Re-Exports by Country, https://www.eia.gov/dnav/ng/ng_move_expc_s1_m.htm, 2019. [Online; accessed 02-August-2019].

[69] British Columbia Clean Energy Act. Greenhouse Gas Reduction (Clean Energy) Regulation, https://www2.gov.bc.ca/gov/content/industry/electricity-alternative-energy/transportation-energies/clean-transportation-policies-programs/greenhouse-gas-reduction-regulation, 2012. [Online; accessed 3-December-2019].

[70] A. S. R. Subramanian, T. Gundersen, T. A. Adams II, Modeling and simulation of energy systems: A review, Processes 6 (2018) 238.

[71] U.S. Energy Information Administration. Short-term energy outlook, https://www.eia.gov/outlooks/steo/report/prices.php, 2019. [Online; accessed 02-August-2019].

[72] Waste today magazine. The US can learn from Sweden, https://www.wastetodaymagazine.com/article/rew0213-sweden-waste-leader/, 2013. [Online; accessed 02-August-2019].